

# Statistical Prediction of Integrated Kinetic Energy in North Atlantic Tropical Cyclones

Michael E. Kozar<sup>1</sup> and Vasubandhu Misra

Center for Ocean-Atmospheric Prediction Studies, Florida State University, Tallahassee, Florida

---

<sup>1</sup> *Corresponding author address: Michael Kozar, Center for Ocean-Atmospheric Prediction Studies, Florida State University, 2000 Levy Avenue, Building A, Suite 292, Tallahassee, FL 32306-2741; email: mkozar@coaps.fsu.edu*

Abstract

1  
2  
3  
4  
5  
6  
7  
8  
9  
10  
11  
12  
13  
14  
15  
16  
17  
18  
19  
20  
21  
22  
23  
24  
25  
26  
27  
28  
29  
30  
31  
32

Integrated Kinetic Energy (IKE) is a useful quantity that measures the size and strength of a tropical cyclone wind field. As a result, it is inherently related to the destructive potential of these powerful storms. In most current operational settings, there are limited resources designed to assess the IKE of a tropical cyclone, as storm track and maximum intensity are typically prioritized. Therefore, to complement existing forecasting tools, a statistical scheme is created to project fluctuations of IKE in North Atlantic tropical cyclones for several forecast intervals out to seventy-two hours. The resulting scheme, named Statistical Prediction of Integrated Kinetic Energy (SPIKE), utilizes multivariate normal regression models trained on environmental and storm-related predictors from all North Atlantic tropical cyclones occurring from 1990 through 2011. During this training interval, SPIKE outperforms persistence and is capable of explaining more than 80% of observed variance in total IKE values at a forecast interval of 12 hours, trailing down to just below 60% explained variance at an interval of 72 hours. The skill of the SPIKE model is evaluated further using bootstrapping exercises in order to gauge the predictive abilities of the statistical scheme. In addition, the performance of the SPIKE model is also evaluated for the 2012 Atlantic Hurricane Season, which notably falls outside of the training interval. Ultimately, the validation exercises return shared variance scores similar to those found in the training exercises, serving as a proof of concept that the SPIKE model can be used to project IKE values when given accurate predictor data.

33 **1. Introduction**

34 Over the past few decades, predicting track and intensity fluctuations of North Atlantic  
35 tropical cyclones (TCs) has been a major emphasis for operational forecasters and atmospheric  
36 researchers alike. Both track and intensity metrics are definitively connected to the risks of a  
37 tropical cyclone, as maximum wind speed (VMAX) is related to the maximum potential  
38 destructiveness of a storm's wind field (e.g. Emanuel 2005; Bell et al. 2000), and storm position  
39 is used to identify the regions at risk of experiencing the storm.

40 Despite the inherent usefulness of track and intensity metrics, they do not yield information  
41 on the size or overall strength of TCs. Over the past few Atlantic hurricane seasons, several  
42 notable landfalling TCs have produced more damage than otherwise would have been expected  
43 by a storm of its intensity. Hurricanes Ike (2008) and Irene (2011) both produced in excess of  
44 \$15 billion in damage across the United States as noted by the National Hurricane Center's  
45 (NHC) tropical cyclone reports (Berg 2009; Avila and Cangialosi 2011) despite being rated as  
46 category two and category one storms respectively at time of landfall on the Saffir Simpson  
47 Hurricane Wind Scale ("SSHWS"; Saffir 1975; Simpson 1974). More recently, Sandy (2012)  
48 only had a VMAX of 70 knots when it made landfall as an extraordinarily large post-tropical  
49 storm, yet it caused in excess of \$50 billion in total damage (Blake et al. 2013). As a result of  
50 these recent damaging storms and those from the record-setting 2005 Atlantic Hurricane  
51 Season (i.e. Hurricane Katrina), some researchers have questioned whether or not intensity  
52 metrics, such as maximum sustained winds, are best suited to communicate the risks of TCs  
53 (Kantha 2006).

54 Hurricanes Ike, Irene, and Sandy were all very large storms despite their weaker intensities.  
55 Therefore, it is distinctly possible that VMAX is not the sole variable tied to damage potential,  
56 especially in large tropical cyclones. Irish et al. (2008) found that storm size is significantly  
57 correlated to storm surge in Atlantic Hurricanes and recommended that although intensity

58 scales adequately categorize wind damage, storm size must be considered to adequately  
59 categorize damage from flooding. Of course, storm surge damage is also significantly  
60 influenced by non-meteorological variables such as coastal bathymetry, population density, and  
61 property value. Nonetheless, with all else being equal, storm size is thought to have a significant  
62 influence over storm surge risks in landfalling TCs. Overall, conclusions such as these  
63 underscore the importance of assessing TC structure in real time and also help to validate the  
64 usefulness of metrics related to TC size such as operational wind radii.

65 Consequently, new scales and metrics have emerged as a complement to the SSHWS that  
66 are more closely tied to the overall kinetic energy of tropical storms (Powell and Reinhold 2007;  
67 Maclay et al. 2008). Integrated kinetic energy (IKE) is one such metric that is calculated by  
68 accumulating one-half of the 10-meter wind field squared ( $U^2$ ) times the density ( $\rho$ ) per unit  
69 volume over a one-meter depth volume domain of a tropical cyclone (Powell and Reinhold  
70 2007), or more specifically,

$$(1) \quad IKE = \int_v \frac{1}{2} \rho U^2 dV .$$

71 In most cases, IKE is integrated using Equation 1 over a portion of the storm volume ( $V$ ) that  
72 contains wind speeds greater than a certain threshold, such as tropical storm force or hurricane  
73 force (Powell and Reinhold 2007; Misra et al. 2013).

74 Importantly, unlike maximum sustained wind metrics, IKE responds to changes in the overall  
75 size, strength, and intensity of a TC. With respect to the physical processes that govern damage  
76 potential, IKE is designed to scale with the stress of the wind on the ocean as well as the wind  
77 load that acts upon a structure (Powell and Reinhold 2007). Therefore, IKE and other similar  
78 kinetic energy metrics are hypothesized to correspond well to the destructive potential of TCs,  
79 particularly with regards to storm surge damage.

80 For example, Hurricanes Ike, Irene, and Sandy at their respective times of landfall in the  
81 United States had extremely high IKE values, despite their low intensities (Figure 1). Just prior

82 to landfall, each of these three storms had IKE values that would rank in the top 7.5% of IKE  
83 values for all hurricane fixes between 1990 and 2011. Sandy, in particular, reached a lifetime  
84 maximum of over 400 TeraJoules (TJ) of IKE just prior to landfall, giving it the second highest  
85 maximum IKE value in any Atlantic TC since 1990. Therefore, it is distinctly possible that  
86 forecasting IKE, as a complement to existing intensity metrics, could help to better assess the  
87 risks of landfalling North Atlantic TCs, particularly for larger and less intense storms such as  
88 these three recent examples.

89 Despite the potential usefulness of real-time IKE updates, there are limited resources  
90 currently available to forecasters that are specifically designed to assess the kinetic energy of a  
91 tropical cyclone. Therefore, we present a statistical model, named Statistical Prediction of  
92 Integrated Kinetic Energy (SPIKE), which can potentially be used in real time for forecasting IKE  
93 fluctuations in North Atlantic TCs. Much like the operational Statistical Hurricane Intensity  
94 Prediction Scheme (SHIPS) used for forecasting VMAX (DeMaria and Kaplan 1994;1999;  
95 DeMaria et al. 2005), SPIKE utilizes a multivariate linear regression model trained on a blend of  
96 environmental and internal storm-driven predictors, in addition to observed persistence metrics,  
97 to predict changes of IKE out to three days in the future.

98

## 99 **2. Data**

### 100 *a. Historical Integrated Kinetic Energy Record*

101 In order to calibrate a statistical regression model for IKE, it is first necessary to obtain a  
102 historical record of IKE that can be used as the calibration model's dependent variable. Gridded  
103 analyses of TC wind fields would be ideal for calculating IKE, but unfortunately datasets like  
104 H\*Wind analyses (Powell et al. 1998) are discontinuous, as they are not available for every six-  
105 hourly storm fix. Alternatively, Powell and Reinhold (2007) developed an approximate set of  
106 stepwise equations to calculate estimates of IKE from operational 34-knot, 50-knot, and 64-knot

107 wind radii, the radius of maximum wind (RMW), and VMAX. This methodology to approximate  
108 IKE from operational wind radii has been used previously to catalogue historical IKE levels  
109 (Misra et al. 2013) and will be used again here to form a large historical record of IKE values to  
110 train and test our statistical model. Specifically, the operational wind radii from the extended  
111 best track dataset (Demuth et al. 2006) are utilized to create a six-hourly record of IKE values  
112 for all North Atlantic TCs over a twenty-two year training interval between 1990 and 2011. The  
113 resulting IKE values in the historical dataset specifically measure the integrated kinetic energy  
114 only over the portion of the wind field where the wind speeds are of tropical storm force or  
115 greater ( $U > 18 \text{ m s}^{-1}$ ). This specific IKE quantity is selected because it is hypothesized to be  
116 closely related to storm surge damage potential by Powell and Reinhold (2007).

117 In total, our historical IKE record comprises of 5498 six-hourly IKE values from 291  
118 individual TCs included from 1990 to 2011 (one IKE value for each six-hourly TC fix). For storm  
119 fixes to be included in this IKE database, the storm must have maximum sustained winds of  
120 tropical storm force or greater, and the storm must be classified as a tropical or subtropical  
121 cyclone in the official best track database (i.e. extratropical and post-tropical lows are not  
122 considered). The vast majority of the fixes that meet these criteria, and are included in the  
123 historical IKE database, are located over the open ocean. However, there are a small minority of  
124 points, for which the center of the TC is located over land. These so called “land points” occur  
125 mostly over islands or very near the coastlines of mainland North America, as storms typically  
126 do not retain tropical characteristics and tropical storm intensity long after landfall. We elected  
127 not to remove these “land points” in order to include landfalling storms in our training sample,  
128 considering that TCs have the most significant societal impacts when they make landfall.

129 The relative frequency distribution of this large sample of six-hourly historical IKE data points  
130 is shown in Figure 1. It is immediately evident that Atlantic TCs most often have IKE values that  
131 do not exceed 25 TJ. The mean IKE value in the dataset is 34.9 TJ, and the standard deviation

132 is 43.0 TJ. In rare instances, TCs can briefly obtain IKE values greater than 300 TJ, typically  
133 near the end of their time as a tropical cyclone.

134 It should be noted that the historical wind radii dataset used to calculate historical IKE  
135 values is subject to year-to-year and storm-to-storm inconsistencies. Landsea and Franklin  
136 (2013) estimated that uncertainties for operational 30-knot, 50-knot, and 64-knot radii were quite  
137 large during the 2010 season. In fact, they estimate that on average the error bars for each radii  
138 estimate could exceed 30% of the mean size for each radii. Overall, they find that the accuracy  
139 of the historical wind radii is limited to the data available in the operational or post-storm  
140 analyses, wherein operational radii measured by aircraft reconnaissance have less uncertainty  
141 than do those measured by just satellite observations. Furthermore, Landsea and Franklin  
142 (2013) indicate that landfalling storms and more intense storms typically have less uncertainty,  
143 as these types of storms are generally observed more frequently and with better equipment,  
144 especially landfalling storms which can be observed from the ground. Therefore, the historical  
145 IKE dataset is likely subject to the same inconsistencies of data quality and quantity that is  
146 evident within the wind radii data in the extended best track data.

147

#### 148 *b. Potential Model Predictors*

149 In addition to the historical record of IKE, a pool of potential predictors must also be created  
150 to establish the relationships that will govern the statistical model. These predictors are carefully  
151 selected based on some of the understood relationships between a storm's environment and  
152 the factors that govern the size, strength, intensity, and ultimately kinetic energy of a TC (e.g.  
153 Gray 1968; McBride 1995; Hill and Lackmann 2009; Maclay 2008; Musgrave et al. 2012).

154 These environmental, storm-specific, and persistence predictors are gathered from a  
155 combination of the NHC best track data set (Jarvinen, 1984) and the SHIPS developmental data  
156 set (DeMaria and Kaplan 1999). The variables derived from the NHC best track data are storm-

157 specific predictors, such as date, position, duration, intensity, and translational storm motion.  
158 The environmental variables, which encompass thermodynamic, dynamic, and moisture related  
159 fields known to affect TC behavior, are taken from the aforementioned SHIPS developmental  
160 dataset (DeMaria and Kaplan 1999). In all, thirty-one predictors were considered for this  
161 regression exercise (Table 1).

162 It should be noted that the SHIPS developmental dataset, from which the environmental  
163 data is obtained, is not a forecast, and instead it utilizes analyses and reanalyses from the  
164 National Centers for Environmental Prediction (NCEP) to provide estimates for the observed  
165 environmental conditions experienced by each storm from genesis to dissipation. Therefore, this  
166 model is trained using a so called “perfect prog” approach (e.g. Neumann 1987; DeMaria,  
167 2010), wherein observations and analyses are used to drive a statistical model. Obviously, an  
168 operational real-time version of SPIKE will require the predictors to be forecasted by numerical  
169 models, since the analyses and reanalyses are not available for future time steps in a real-time  
170 operational setting. Therefore, the SPIKE models discussed for the remainder of Sections 3-5,  
171 all of which utilize observations and SHIPS developmental data, are not meant to be forecasts  
172 or even hindcasts. Instead these regression models will provide an estimate for the maximum  
173 potential skill of SPIKE in the idealistic scenario that the forecasted predictors exactly match the  
174 future observations.

175

### 176 **3. Regression Methodology**

177 The distribution of historical six-hourly IKE values is decidedly non-Gaussian as shown in  
178 Figure 1. In fact, the six-hourly total IKE values are approximately log-normally distributed,  
179 which is similar to the distribution of storm size as measured by the radii of vanishing winds  
180 (Dean et al. 2009). Therefore, it would be inappropriate to use linear regression to model total  
181 IKE values. Instead, SPIKE will seek to predict changes of IKE from initial time out to twelve



182 evenly-spaced time intervals from six hours to seventy-two hours (0-6hrs, 0-12hrs, ... , 0-72hrs).  
183 Ultimately, these IKE changes are more normally distributed (e.g. Figure 2), and thus, it  
184 becomes more appropriate to use multivariate linear regression. However, in order to create a  
185 model for each of these twelve forecast intervals, SPIKE regression models must be calibrated  
186 and validated separately for each forecast interval.

187 Based on the success of the statistical SHIPS model used to predict intensity change  
188 relative to other statistical and dynamical models (DeMaria et al. 2005), we utilize similar  
189 regression methodology to construct our SPIKE model for IKE changes. As done by DeMaria  
190 and Kaplan (1994), both the dependent and independent variables are normalized prior to  
191 training the regression model. Ultimately, by normalizing the predictors, it becomes possible to  
192 make a comparison between regression coefficients for various predictors and forecast hours  
193 (DeMaria and Kaplan 1994).

194 To avoid over fitting in our SPIKE regression model, predictor screening must be utilized.  
195 Once again, we follow the lead of DeMaria and Kaplan's SHIPS model (1994; 1999) by using  
196 backwards screening to objectively select the most skillful predictors. Backward predictor  
197 screening is done here by training the model upon all of the predictors for each forecast interval,  
198 and then repeatedly removing the single predictor with the least significant regression coefficient  
199 one at a time, until all of the remaining regression coefficients are significant at the  $p=0.01$  level.  
200 Ultimately, this backward screening methodology retains a smaller subset of predictors that are  
201 used in the SPIKE model for each forecast interval. To make the SPIKE prediction model as  
202 uniform as possible across the forecast intervals, the same predictors are chosen for all  
203 intervals. These predictors are selected if their coefficients are significant at the 99% level for at  
204 least half of the forecast intervals. As a result, predictors may be used on intervals when their  
205 coefficients are not significant, but as pointed out by DeMaria and Kaplan (1994), when a  
206 predictor is not significant, its coefficient becomes small and its influence on the regression  
207 model is diminished.

208 It should also be noted that some of the SHIPS predictors included in Table 1 have missing  
209 or null data values scattered throughout our training interval of 1990-2011. Most notably, some  
210 of the subsurface ocean predictors (i.e. RD26) are unavailable for entire years at the beginning  
211 of the record. Therefore, to account for the limited number of missing predictor values, the  
212 regression coefficients are calibrated and the predictors are screened using a sample of all  
213 storm fixes that contain no missing data in the training interval. In other words, if a certain storm  
214 fix contains even one missing predictor, that data point will not be used in the calibration of the  
215 model. However, once the predictors are chosen and the coefficients are calculated, we  
216 estimate IKE for every storm fix to evaluate model skill. In the case that a predictor is missing,  
217 as occurs occasionally in an operational setting, we filled the missing data point with a value  
218 equivalent to the sample mean (i.e. exactly zero since the predictors are all normalized).

219

## 220 **4. Results**

221 This section presents the results of the SPIKE regression model. In addition to estimating  
222 fluctuations of IKE, SPIKE will also be adapted to estimate total IKE by incorporating  
223 persistence values of kinetic energy. An emphasis will be made in interpreting the physical  
224 relationships that drive the regression model in the first section, because a statistical  
225 relationship is meaningless without an understanding of the underlying physical processes.  
226 Later sections focus on evaluating the calibration and predictive skill of SPIKE with explained  
227 variance and mean error statistics as well as a standard bootstrapping exercise. Finally, the last  
228 section analyzes SPIKE's ability to project IKE values during the 2012 Atlantic Hurricane season  
229 in order to evaluate the model's skill on a season that is outside of the training interval.

230

### 231 *a. Physical Interpretation of Selected Predictors*

232 The predictors retained through the backward screening exercise are shown in the first  
233 column of Table 2. These predictors encompass a wide array of variables ranging from  
234 thermodynamical fields such as the depth of the 26°C isotherm to positional variables such as  
235 latitude, dynamical values like upper-level divergence, and persistence variables such as past  
236 values of IKE. For the sake of simplicity, the variables are referenced as they are abbreviated in  
237 Table 1 for the rest of this discussion.

238 The coefficients for these variables at selected forecast intervals are also shown in Table 2.  
239 Encouragingly, the sign of most of the predictors' coefficients do not vary with forecast hour. For  
240 example, the coefficient for PIKE is negative in all intervals suggesting that storms with higher  
241 IKE are more likely to have decreasing IKE over time. As seen in the distribution of historical  
242 IKE values, TCs most often have low values of IKE; therefore it is not terribly surprising that  
243 higher IKE storms typically weaken. The physical reasoning behind this relationship is tied to the  
244 timing of maximum IKE during a TC lifecycle. As found by Musgrave et al. (2012), TCs often  
245 exhibit storm growth (increasing IKE) through most of their lifecycle. North Atlantic TCs, in  
246 particular, maintain or increase their size even after reaching maximum intensity (Knaff et al.  
247 2014). As a result, TCs often have their highest levels of IKE late in their lifecycle, either prior to  
248 landfall or during extratropical transition (ET) when TCs often undergo wind field expansion as  
249 the RMW moves outward and the outer wind field accelerates (Evans and Hart 2008).  
250 Obviously following landfall or the completion of ET, TCs typically weaken drastically over the  
251 hostile environments of land or the cold northern Atlantic Ocean. Therefore, the negative  
252 coefficient of PIKE can be attributed to the negative IKE change of these strong storms, and the  
253 fact that weaker storms near genesis typically will gain IKE as they become more mature,  
254 provided the environment is not too unfavorable. Similar to PIKE, PDAY has negative  
255 coefficients for all forecast intervals. The negative coefficient is tied to the fact that TCs are  
256 more likely to have periods of increasing IKE close to the peak of the season (small PDAY),  
257 when conditions are typically most favorable for TC development.

258 The only predictor to have a coefficient that changes sign with forecast hour is dIKE12,  
259 wherein the coefficient is positive in the shorter forecast intervals and slightly negative in the  
260 longer intervals. The positive dIKE12 coefficients in the first several forecast intervals make  
261 sense, as storms typically continue to have increasing IKE in most phases of their lifecycle  
262 (Musgrave et al. 2012), wherein a growing storm will continue to grow provided the environment  
263 remains somewhat favorable. Likewise, if a storm is in an environment unfavorable for IKE  
264 growth, the kinetic energy will likely continue to drop, at least in the short term. The slightly  
265 negative sign for the longer forecast intervals is more difficult to reason physically, but it should  
266 be noted that the coefficient is not significant to begin with, suggesting that past 12hr IKE  
267 change is only helpful for determining upcoming IKE changes in the immediate future.

268 In terms of the environmental predictors, some of the underlying physical relationships are  
269 immediately apparent. For example, the coefficients for VORT and D200 are positive,  
270 suggesting a direct relationship between storm growth and each of these fields. In this case,  
271 both low-level vorticity and upper-level divergence are well known conditions that are generally  
272 favorable for large scale organized convection and the formation and development of TCs (e.g.  
273 McBride 1995). Similarly, the negative coefficients for MSLP and PENV are expected, as a  
274 more intense storm and/or a storm with a larger area of low pressure will typically have higher  
275 wind speeds and increased IKE with all else being equal. Likewise, the positive coefficients for  
276 RD26 are unsurprising, as TCs induce turbulent mixing and upwelling in the upper levels of the  
277 ocean which cools SSTs through the entrainment of cooler subsurface waters (e.g. Price 1981).  
278 This SST cooling mechanism plays a significant role of slowing down TC growth and  
279 intensification, especially for slower moving storms over shallow oceanic mixed layers (Schade  
280 and Emanuel 1999). Thus, an environment with a deeper thermocline, and a higher RD26, is  
281 more resistant to the negative SST feedback mechanism, making storm growth more favorable.  
282 Finally, the positive coefficients for DTL also make sense, as TCs tend to weaken as they  
283 approach and eventually cross landmasses.

284 In some cases, however, the physical processes that govern the regression coefficients are  
285 less apparent. For example, the positive coefficients for SHRD and LAT seem somewhat  
286 counterintuitive to conventional TC development theories, wherein TCs favor low shear  
287 environments as well as warmer oceans which are typically found in the lower latitudes.  
288 However, as discovered by Maclay et al. (2008), TC growth can also be tied to external forcing  
289 from trough interactions and baroclinic environments over the higher latitudes. The positive  
290 coefficients for REFC, for example, reflect the positive influence of trough interactions on storm  
291 growth (Maclay et al. 2008; DeMaria et al. 1993). Likewise, the positive coefficients of LAT and  
292 SHRD are likely related to ET. Historically, ET occurs in just under half of all Atlantic TCs (Hart  
293 and Evans 2001), typically over the more sheared higher latitudes of the basin. Thus the wind  
294 field expansion from ET and the subsequent increase in IKE over the higher latitudes is likely  
295 influencing the signs of these coefficients. Finally, the negative coefficients for RHLO are  
296 particularly counterintuitive because in most cases increased low level humidity is favorable for  
297 TC development and also for increased storm size (e.g. Hill and Lackmann 2009). However, this  
298 apparent contradiction can be explained going back to the relationship between increasing IKE  
299 and extratropical transition, whereas storms undergoing ET often have an intrusion of dry air  
300 into the storm circulation (Jones et al. 2003), thus decreasing RHLO. Therefore, it is possible  
301 that lower RHLO could be associated with expanding wind fields in ET or other similar events,  
302 but additional study of the physical relationship between IKE and RHLO is clearly warranted.

303

#### 304 *b. Model Skill and Validation Tests, 1990-2011*

305 The shared variance between the SPIKE model and IKE variability is shown for selected  
306 forecast intervals during the training period in Table 2. As is the case with SHIPS (DeMaria and  
307 Kaplan 1994), the explained variance increases with increasing forecast hour. At first, this  
308 appears counterintuitive as forecast skill typically decreases with lead time. However, the

309 average magnitude of IKE change from 1990 to 2011 is much smaller in the shorter forecast  
310 intervals than in the larger forecast intervals (9 TJ for 12hr; 32 TJ for 72hr). Considering the  
311 errors and biases within the historical archive of operational wind radii, the calculations for  
312 observed IKE likely contain biases on the same order as, or even greater than, the IKE changes  
313 themselves for the shorter forecast intervals. Therefore, the model will perform poorly at  
314 explaining these smaller short-term changes that are dominated by observational biases.  
315 Furthermore, the predictors used to train SPIKE in this “perfect prog” approach are observed  
316 and not forecasted. Therefore, this exercise is not hurt by forecast biases and errors, which  
317 would ostensibly increase with forecast hour. Instead this exercise is a proof of concept for  
318 forecasting IKE changes given idealistic perfectly forecasted predictors.

319 The shared variance scores of SPIKE for predicting integrated kinetic energy changes are  
320 all significant considering the large sample sizes from using thousands of storm fixes between  
321 1990 and 2011. The shared variance statistics for SPIKE are particularly impressive at the  
322 longer forecast intervals ( $r^2 = 0.54$ ), where they approach and in some cases exceed the shared  
323 variance levels for SHIPS and TC intensity (DeMaria and Kaplan 1994; 1999). Admittedly, the  
324 model performs quite poorly in the shorter ranges, especially considering observed predictors  
325 are used instead of forecasted predictors.

326 Although SPIKE is designed to predict the normally distributed quantity of integrated kinetic  
327 energy change, it can still be adapted to predict total IKE values (Figure 3). This is done by  
328 adding the estimate of IKE change from SPIKE to the known persistence IKE value. As a result  
329 of incorporating persistence into the IKE forecast, the shared variance levels between SPIKE’s  
330 total integrated kinetic energy estimates are significantly higher than its estimates for just IKE  
331 fluctuations. At a forecast interval of 12hrs, SPIKE can estimate total IKE with a staggering  
332 explained variance of 84%. This shared variance drops off to 70% by 30 hours and a still  
333 impressive 60% by a forecast interval of 72 hours (Figure 4a).

334 The use of persistence to obtain total IKE projections allows the SPIKE products to take  
335 advantage of the inertial nature of IKE quantities. Whereas a point metric like maximum  
336 sustained wind can and does change rapidly somewhat regularly (e.g. Kaplan and DeMaria  
337 2003), kinetic energy integrated across the entire wind field does not change as rapidly.  
338 Although drastic intensity changes do impact IKE values, rapid intensification (RI) events  
339 typically result in a drastic increase of near surface winds over a small confined area of  
340 convection near the center of the storm. Therefore, the impact on IKE during RI is typically  
341 small, provided the overall size of the storm's wind field remains somewhat constant. Therefore,  
342 a persistence forecast of total IKE is typically very skillful, especially in a short forecast interval.  
343 However, at longer forecast intervals, persistence does not fare nearly as well ( $r^2 = 25\%$  at  
344 72hrs; Figure 4a). In fact, the SPIKE regression model is more skillful at estimating total IKE  
345 values at a 72-hour forecast interval than is persistence at forecasting the same quantity on a  
346 much shorter 30-hour interval. The lack of skill by persistence over time indicates that  
347 environmental and storm-specific data must be utilized for longer-term forecasts of IKE.

348 Absolute mean errors were also calculated for the total SPIKE model by computing the  
349 average magnitude of the differences between the SPIKE forecast and the observed total IKE  
350 values for each of the storm fixes in the 1990-2011 training interval. These mean errors for the  
351 total SPIKE model and for a persistence forecast are plotted in Figure 4b. It should be noted  
352 that the mean errors for the persistence forecast are equal to the mean magnitude of IKE  
353 change for each forecast interval since a persistence forecast by definition will predict a change  
354 of zero TJs. Therefore, the mean magnitude of errors for the SPIKE model's total IKE  
355 projections are of the same magnitude as the IKE changes themselves within the shortest  
356 forecast intervals (e.g. ~10 TJ for the 12 hour forecast interval; ~15 TJ for the 24 hour forecast  
357 interval). This ultimately means that a short-term total IKE forecast is not significantly better than  
358 persistence. While unfortunate, this does not come as a surprise, as SPIKE has low shared  
359 variance scores in these shorter forecast windows for predicting the more subtle IKE changes

360 (Table 2). However, a persistence forecast has significantly more error than does the SPIKE  
361 model in forecast intervals greater than 24 hours. In fact, at a forecast window of 48 hours, total  
362 IKE projections from SPIKE have a mean error magnitude of 18.6 TJ compared to a much  
363 higher 24.2 TJ from a persistence forecast. Therefore, the mean error statistics support the  
364 conclusions drawn from the shared variance statistics, wherein persistence is a tough forecast  
365 to beat within 24 hours and the SPIKE model exhibits significant skill over persistence beyond  
366 that point.

367 Analysis of mean squared error (MSE) values in the SPIKE model, with respect to those  
368 from a persistence forecast, further emphasize that SPIKE offers a significant skill improvement  
369 over a persistence forecast during the training interval (Figure 5). In a twelve-hour forecast  
370 window, SPIKE exhibits a 14% reduction of MSE values when compared to a persistence  
371 forecast. Two-sample bootstrapping tests using the squared errors of the SPIKE model and a  
372 persistence forecast suggest that SPIKE's improvement over persistence is not quite significant  
373 at the one-sided  $p=0.10$  level for this short forecast window. However, at 30 hours, SPIKE  
374 exhibits a 36% improvement over a persistence forecast in terms of MSE, which is significant at  
375 the  $p=0.01$  level according to two-sample bootstrapping tests. The percent decrease of MSE in  
376 the SPIKE model relative to persistence within the training interval continues to improve across  
377 all later forecast intervals, culminating in a 60% reduction of MSE in the 72-hour SPIKE model  
378 compared to a 72-hour persistence forecast.

379 In addition to simply calculating statistics over the calibration interval, some validation  
380 exercises are also performed using standard bootstrapping techniques. These bootstrapping  
381 exercises are done by training the model over a sample that is created by randomly selecting  
382 data points from the overall population of IKE and predictor data (repetition allowed). The  
383 regression coefficients from the model trained over this sample are then used over the original  
384 population to examine how much skill is lost. In the case of the SPIKE model for kinetic energy  
385 change, there is an average decrease in shared variance of 3.7% across all twelve of the



386 forecast intervals. The decrease of skill for the total kinetic energy estimates is less significant,  
387 averaging less than 0.5% across all of the forecast intervals. Ultimately, these simple tests  
388 indicate that SPIKE should be able to retain predictive skill when using a different sample of  
389 data. However, once again, it should be noted that because developmental SHIPS data is used  
390 for the predictors, there likely will be a decrease in skill when using forecasted predictors in an  
391 operational setting.

392

### 393 *c. Model Performance in the 2012 Atlantic Hurricane Season*

394 The 2012 Atlantic Hurricane Season consisted of 19 tropical cyclones, ten of which were  
395 hurricanes and two that eventually reached major hurricane status. A total of 395 storm fixes  
396 were taken from the extended best track dataset to estimate IKE for each storm. Similar to  
397 storms in the training interval from 1990 to 2011, the TCs of the 2012 Atlantic season had IKE  
398 values less than 25 TJ for most of their lifetimes. However, four storms (Hurricanes Leslie,  
399 Nadine, Rafael, and Sandy) all obtained in excess of 100 TJs of IKE, mostly in the latter stages  
400 of their lifecycles over the middle and upper latitudes of the basin.

401 The same SPIKE models that were calibrated on the 1990-2011 data in the previous  
402 sections (coefficients listed in Table 2) are utilized to project observed fluctuations of IKE during  
403 the 2012 Atlantic Hurricane Season, as means of determining SPIKE's potential predictive skill  
404 outside of the training interval. Predictor data for the 2012 season is once again taken from the  
405 best track dataset (Jarvinen, 1984) and the SHIPS developmental data set (DeMaria and  
406 Kaplan 1999). Therefore, this analysis, which does not use dynamically forecasted predictors, is  
407 not meant to assess the operational skill of SPIKE. Instead, this exercise serves as an  
408 evaluation of SPIKE's skill outside of the training interval when given idealistically accurate  
409 predictors.

410 Overall, the SPIKE model exhibits comparable skill during the 2012 season when  
411 compared to the 1990-2011 training interval. The explained variance and mean absolute  
412 forecast errors are shown in Figure 6. SPIKE explains an even higher percentage of the  
413 observed total IKE variance in 2012 when compared to the training interval. At a forecast  
414 interval of 36 hours, the 2012 SPIKE model explains an astonishing 83% of the variance of total  
415 IKE values, as compared to the 67% explained by SPIKE during the longer training interval. The  
416 main reason for this apparent enhanced skill during the 2012 season, when compared to the  
417 longer training interval, likely stems from the fact that persistence corresponds extremely well  
418 with future IKE values during the 2012 season. In fact, out to 36 hours, a simple persistence  
419 forecast explains more than 80% of the variance during the 2012 season, suggesting that the  
420 kinetic energy levels of TCs during this one season were even more inertial than should be  
421 expected on average.

422 In terms of mean absolute errors, SPIKE does not appear to perform as well during the  
423 2012 season when compared to the 1990-2011 training interval (Figure 6b). An increase in  
424 forecast error should be expected since the 2012 data was not in the training interval that was  
425 used to calibrate the regression coefficients in SPIKE. In this case, the error at a forecast  
426 window of 72 hours was 29.2 TJs during the entire 2012 season, which is a staggering 36%  
427 higher than the mean 72-hour error during the 22-year training interval. The highest SPIKE  
428 errors during the 2012 season unsurprisingly occurred during Hurricane Sandy. As previously  
429 mentioned, Sandy had near-record levels of IKE near the end of its lifecycle. The SPIKE model,  
430 at all forecast intervals, correctly projected that Sandy would have IKE levels above 150 TJs  
431 before reaching the Mid-Atlantic coastline. This forecasted level of IKE from SPIKE would have  
432 placed Sandy within the top 2.5% of all TC fixes during the training interval. Therefore, in many  
433 regards, the SPIKE forecast still would have been more than adequate to categorize the high  
434 damage potential of Sandy, which explains why the shared variance score of SPIKE during the  
435 2012 season is not similarly worse than the training interval shared variance levels.

436 Nonetheless, SPIKE was unable to project that Hurricane Sandy would reach near-record IKE  
437 values exceeding 400 TJs. As a result, even a very high forecast of 300 TJ for Sandy would  
438 contain an enormous error magnitude of more than 100 TJs, contributing to the much higher  
439 than expected mean error levels shown in Figure 6b.

440 If the final dozen storm fixes of Hurricane Sandy were neglected, the SPIKE model  
441 would have significantly less mean error during the 2012 season (Figure 6b). In fact, the mean  
442 error during 2012, excluding these Sandy data points, would be strikingly similar to the mean  
443 errors during the full 22-year training interval at all forecast intervals. Mean squared error  
444 statistics (Figure 7) tell a similar story, wherein the SPIKE model improves upon a persistence  
445 forecast during the 2012 season, excluding Sandy, for all forecast hours. Like the MSE  
446 reduction analysis done for the training interval in Section 4b, SPIKE performs increasingly  
447 better than persistence with increasing lead time. The percent reduction of MSE in SPIKE  
448 relative to persistence becomes significant at the one-sided  $p=0.05$  level at a forecast interval of  
449 48-hours, where SPIKE has 35% less MSE than a persistence forecast. At a forecast interval of  
450 72-hours, SPIKE has a reduction of MSE relative to persistence of nearly 45% during the 2012  
451 season, excluding Sandy.

452 Overall, this exercise suggests that the SPIKE model performs well over a validation  
453 dataset such as the 2012 season. Skill relative to persistence increases with increasing lead  
454 time, as expected. Within a twenty-four hour forecast window, the high correspondence  
455 between SPIKE projections and historical IKE in 2012 can be attributed to the skill of a short-  
456 term IKE persistence forecast. However, outside of this one-day forecast interval, the SPIKE  
457 model performs significantly better than a persistence forecast in this validation exercise.

458

## 459 **5. Conclusions**

460 Although kinetic energy forecasts are uncommon in operations today, IKE is a metric that  
461 could be potentially very useful to forecasters. The relationship between kinetic energy metrics  
462 and the storm surge damage potential of a tropical cyclone makes forecasting this physical  
463 quantity very desirable, especially since IKE better represents damage potential in larger storms  
464 such as Sandy than does VMAX. On the other hand, it should be noted that one weakness of  
465 kinetic energy metrics is their underestimation of wind damage in smaller but intense storms  
466 such as Charley in 2004 (Maclay et al. 2008). Therefore, it is suggested that IKE forecasts  
467 should be used in conjunction with existing VMAX forecasts to maximize a forecaster's ability to  
468 assess the wide array of risks for damage in landfalling storms.

469 The simple statistical regression model designed here adequately estimates changes of IKE  
470 in Atlantic TCs out to 72 hours. More specifically, the model created here explains as much as  
471 50% of the variance in historical IKE changes out to three days. More impressively, it is found  
472 that persistence can be added to SPIKE's forecast for IKE change to successfully project total  
473 values of IKE. In this regard, SPIKE can explain more than 80% of the observed variance in  
474 historical total IKE values at a 12-hour forecast interval, trailing down to near 60% at 72 hours.  
475 The increase in skill for projecting total IKE is attributed to the inertial nature of the IKE metric.  
476 The fact that persistence is a viable kinetic energy forecast in the short term could be used to  
477 the advantage of forecasters in assessing TC risks, especially considering the lack of recent  
478 improvements in forecasting the less persistent and notoriously challenging intensity metrics  
479 (Rappaport et al. 2009).

480 Validation tests suggest that SPIKE's high levels of skill should not degrade sharply when  
481 used in a forecast environment, provided that the predictors are forecasted accurately. For  
482 example, bootstrapping exercises revealed that SPIKE remains skillful at projecting total IKE  
483 values in historical storms, even when calibrated by resampled data. Furthermore, validation of  
484 SPIKE during the 2012 season reveals that the model can perform reasonably well when given  
485 predictor data outside of its training interval, as will be required in an operational setting.

486 However, it should be once again noted that none of these exercises used forecasted  
487 predictors. Thus, it is fair to expect SPIKE to have somewhat reduced skill levels in a truly  
488 operational setting because the predictors will be imperfectly forecasted for future time steps in  
489 nearly all scenarios.

490 Previous work done by DeMaria (2010) offers some insight with regards to the amount of  
491 skill that could be lost by moving from a “perfect prog” approach to an operational approach with  
492 imperfectly forecasted predictors. DeMaria (2010) found that the skill of a statistical-dynamical  
493 model, such as the Logistic Growth Equation Model (LGEM), did not drastically improve when  
494 given perfect large-scale environmental predictors. Since most of the predictors in our SPIKE  
495 model are indeed large-scale environmental predictors, this bodes well for the potential skill of  
496 the SPIKE model in an operational setting. However, DeMaria (2010) noted that smaller scale  
497 predictors that are more dependent upon track are more likely to affect model skill when moving  
498 from a “perfect prog” approach to an operational approach with forecasted predictors. This is  
499 relevant to SPIKE, as MSLP is used in our model. The intensity of a TC obviously is quite  
500 dependent on storm track, especially when a storm is nearing a coastal environment.

501 Considering that MSLP is an important predictor in the SPIKE model, it is worthwhile to examine  
502 how an imperfect estimation of MSLP will affect the skill of SPIKE. Therefore, we replaced the  
503 observed MSLP predictor in our “perfect prog” approach with an MSLP persistence forecast,  
504 leaving all other “perfect” predictors the same. In most cases, a persistence forecast of MSLP  
505 will be a poor indication of future MSLP values, as TC intensity tends to change somewhat  
506 rapidly, particularly when storms near landfall. Nonetheless, the skill of the SPIKE model  
507 decreases by no more than 20% across all forecast intervals, in terms of both explained  
508 variance and MSE, when the poor persistence MSLP predictor is used in place of the “perfect”  
509 observed MSLP predictor used throughout the previous sections. In fact, a SPIKE model trained  
510 with an MSLP persistence predictor is still significantly better at projecting integrated kinetic  
511 energy than an IKE persistence forecast at the one-sided  $p=0.10$  level in the training interval for

512 all forecast intervals exceeding 24 hours. This further suggests that the SPIKE model will likely  
513 offer an improvement over a persistence forecast of IKE, even when using imperfect operational  
514 predictors.

515 In summary, this exercise serves as a proof of concept that when given accurately  
516 forecasted predictors, it is possible to project IKE in an operational setting. This work can be  
517 built upon by using IKE forecasts to statistically estimate storm size and wind field distribution.  
518 Future work will also be focused on adapting this model into a dynamical-statistical model that  
519 can be used in real time, while also continuing to build upon our understanding of the underlying  
520 physical processes that control kinetic energy variability.

521

522

523

524

525

526

## 527 **Acknowledgements**

528 Thanks to Drs. Mark Powell, Robert Hart, Phillip Sura, Allan Clarke, Ming Ye, T.N. Krishnamurti,  
529 and James O'Brien for their helpful comments and feedback. In addition, we greatly appreciate  
530 the helpful comments provided to us during the review process by Dr. Mark DeMaria and an  
531 anonymous reviewer. This work was supported by grants from NOAA (NA12OAR4310078,  
532 NA10OAR4310215, NA11OAR4310110), and USDA (027865).

533

534

535

536 **References**

537  
538  
539 Avila L.A. and J. Cangialosi, 2011: Tropical Cyclone Report Hurricane Irene (AL092011) 21-28  
540 August 2011. *National Hurricane Center*. [available online: [http://www.nhc.noaa.gov/data/tcr/](http://www.nhc.noaa.gov/data/tcr/AL092011_Irene.pdf)  
541 [AL092011\\_Irene.pdf](http://www.nhc.noaa.gov/data/tcr/AL092011_Irene.pdf)]

542  
543 Bell, G. D., and Coauthors, 2000: Climate assessment for 1999. *Bull. Amer. Meteor. Soc.*,81,  
544 1328–1378.

545  
546 Berg, R., 2009: Tropical Cyclone Report Hurricane Ike (AL092008) 1-14 September 2008.  
547 *National Hurricane Center*. [available online: [http://www.nhc.noaa.gov/pdf/TCR-](http://www.nhc.noaa.gov/pdf/TCR-AL092008_Ike_3May10.pdf)  
548 [AL092008\\_Ike\\_3May10.pdf](http://www.nhc.noaa.gov/pdf/TCR-AL092008_Ike_3May10.pdf)].

549  
550 Blake, E.S., T.B. Kimberlain, R.J. Berg, J.P. Cangialosi, and J.L. Bevin II, 2013: Tropical  
551 Cyclone Report Hurricane Sandy (AL182012) 22-29 October 2012. *National Hurricane*  
552 *Center*. [available online: [http://www.nhc.noaa.gov/data/tcr/AL182012\\_Sandy.pdf](http://www.nhc.noaa.gov/data/tcr/AL182012_Sandy.pdf)]

553  
554 Dean. L., K.A. Emanuel, and D.R. Chavas, 2009: On the size distribution of Atlantic tropical  
555 cyclones. *Geophys. Res. Lett.*, 36, L14803.

556  
557 DeMaria, M., and J. Kaplan, 1994: A statistical hurricane intensity prediction scheme (SHIPS)  
558 for the Atlantic basin. *Wea. Forecasting*, 9, 209 220.

559  
560 —, and —, 1999: An updated statistical hurricane intensity prediction scheme (SHIPS) for  
561 the Atlantic and eastern north Pacific basins. *Wea. Forecasting*, 14, 326-337.

562

563 —, M. Mainelli, L.K. Shay, J.A. Knaff and J. Kaplan, 2005: Further Improvements in the  
564 Statistical Hurricane Intensity Prediction Scheme (SHIPS). *Wea. Forecasting*, **20**, 531-543.  
565

—, J-J. Baik, and J. Kaplan, 1993: Upper-level eddy angular momentum fluxes and tropical  
cyclone intensity change. *J. Atmos. Sci.*, **50**, 1133–1147.

—, 2010: Tropical Cyclone Intensity Change Predictability Estimates Using a Statistical-  
Dynamical Model, *29<sup>th</sup> Conf. on Hurr. And Trop. Meteor., May 10-14, Tuscon, AZ, Amer.  
Meteor. Soc., 9C.5.*

566

567 Demuth, J.L., M. DeMaria., and J. A. Knaff, 2006: Improvement of advanced microwave  
568 sounder unit tropical cyclone intensity and size estimation algorithms. *J. Appl. Meteorol.  
569 Climatol.*, **45**, 1573-1581.

570

571 Emanuel, K., 2005: Increasing destructiveness of tropical cyclones over the past 30 years.  
572 *Nature*, **436**, 686–688.

573

574 Evans, C., and R.E. Hart, 2008: Analysis of the Wind Field Evolution Associated with the  
575 Extratropical Transition of Bonnie (1998). *Mon. Wea. Rev.*, **136**, 2047-2065.

576

577 Gray, W. M., 1968: Global view of the origins of tropical disturbances and storms. *Mon. Wea.  
578 Rev.*, **96**, 669-700.

579

580 Hart R.E., and J.L. Evans, 2001: A Climatology of the Extratropical Transition of Atlantic  
581 Tropical Cyclones. *J. Climate*, **14**, 546-564.

582



583 Hill, K.A., and G.M. Lackmann, 2009: Influence of Environmental Humidity on Tropical Cyclone  
584 Size. *Mon. Wea. Rev.*, **137**, 3294–3315.

585

586 Irish, J.L., D T. Resio, and J.J. Ratcliff, 2008: The influence of Storm Size on Hurricane Surge.  
587 *J. Phys. Oceanogr.*, **38**, 2003-2013.

588

589 Jarvinen, B. R., C. J. Neumann, and M. A. S. Davis, 1984: A tropical cyclone data tape for the  
590 North Atlantic Basin, 1886-1983: Contents, limitations, and uses. NOAA Technical  
591 Memorandum NWS NHC 22, Coral Gables Florida, 21 pp.

592

593 Jones, S.C., and Coauthors, 2003: The Extratropical Transition of Tropical Cyclones: Forecast  
594 Challenges, Current Understanding, and Future Directions. *Wea. Forecasting*, **18**, 1052–  
595 1092.

596

597 Kantha, L., 2006: Time to replace the Saffir-Simpson Hurricane Scale? *Eos, Trans. Amer.*  
598 *Geophys. Union*,**87**,3–6.

599

600 Kaplan, J., and M. DeMaria, 2003: Large-Scale Characteristics of Rapidly Intensifying Tropical  
601 Cyclones in the North Atlantic Basin. *Wea. Forecasting*, **18**, 1093–1108.

602

603 Knaff, J.A., S.P. Longmore, D.A. Molnar, 2014: An Objective Satellite-Based Tropical Cyclone  
604 Size Climatology, *J. Climate*, **27**, 455-476.

605

606 Landsea, C.W., and J.L. Franklin, 2013: Atlantic Hurricane Database Uncertainty and  
607 Presentation of a New Database Format. *Mon. Wea. Rev.*, **141**, 3576-3592.

608

609 Maclay K.S., M. DeMaria, and T.H. Vonder Haar, 2008: Tropical Cyclone Inner-Core Kinetic  
610 Energy Evolution. *Monthly Weather Review* **136**:12, 4882-4898.  
611

612 McBride, J. L., 1995: Tropical cyclone formation. *Global Perspectives on Tropical Cyclones*,  
613 WMO/TD No. 693, Rep. TCP-38, World Meteorological Organization, 63–105.  
614

615 Misra V., S. DiNapoli, and M. Powell, 2013: The Track Integrated Kinetic Energy of Atlantic  
616 Tropical Cyclones. *Monthly Weather Review* **141**:7, 2383-2389.  
617

618 Musgrave K.D., R. K.Taft, J. L.Vigh, B. D.McNoldy, and W. H.Schubert, 2012: Time evolution of  
619 the intensity and size of tropical cyclones, *J. Adv. Model. Earth Syst.*, **4**, M08001.  
620

621 Neumann, C.J., 1987: Prediction of tropical cyclone motion: Some practical aspects. Extended  
622 Abstracts, *17<sup>th</sup> conference on Hurr. And Trop. Meteor.*, April 7-10, 1987, Miami, FL., Amer.  
623 Meteor. Soc., 266-269.  
624

625 Price, J.F., 1981: Upper Ocean Response to a Hurricane. *J. Phys. Oceanogr.*, **11**, 153–175.  
626

627 Powell, M.D., and T.A. Reinhold, 2007: Tropical Cyclone Destructive Potential by Integrated  
628 Kinetic Energy. *Bull. Amer. Meteor. Soc.*, **88**, 513–526.  
629

630 —, S.H. Houston, L. R. Amat, and N. Morisseau-Leroy, 1998: The HRD real-time hurricane  
631 wind analysis system. *J. Wind Eng. Ind. Aerodyn.*, **77–78**, 53–64.  
632

633 Rappaport, E.N., and Coauthors, 2009: Advances and Challenges at the National Hurricane  
634 Center. *Wea. Forecasting*, **24**, 395-419.

635  
636  
637  
638  
639  
640  
641  
642  
643  
644  
645  
646  
647  
648  
649  
650  
651  
652  
653  
654  
655  
656  
657  
658  
659  
660  
661  
662  
663  
664  
665  
666  
667  
668  
669

Saffir, H., 1975: Low cost construction resistant to earthquakes and hurricanes. *ST/ESA/23, United Nations*, 216 pp.

Schade L.R. and K.A. Emanuel, 1999: The Ocean’s Effect on the Intensity of Tropical Cyclones: Results from a Simple Coupled Atmosphere–Ocean Model. *J. Atmos. Sci.*, **56**, 642–651.

Simpson, R. H., 1974: The hurricane disaster potential scale. *Weatherwise*, **27**, 169–186.

## 670 **Figure Captions**

671

672 **Figure 1:** Relative frequency distribution of six-hourly VMAX (panel A) and IKE (panel B)  
673 measurements in Atlantic TCs between 1990 and 2011. This sample includes 5498 fixes from  
674 291 storms. Vertical lines are shown to indicate VMAX and IKE values for selected hurricanes  
675 just prior to a US landfall. The times of these IKE measurements are as follows: Ike 9/13/08  
676 00Z; Irene 8/28/11 06Z; Sandy 10/29/12 18Z. The three storm points would fall in the top 45% of  
677 all TCs points in terms of VMAX and the top 7.5% of TCs in terms of IKE from 1990 through  
678 2011.

679

680 **Figure 2:** Relative frequency distribution of 0-24 hour IKE changes (panel A), and normalized 0-  
681 24 hour IKE changes (panel B). The normalized changes of IKE at various forecast times is  
682 used as the target predictand for the linear SPIKE regression models

683

684 **Figure 3:** Scatter plot of observed total IKE values vs. estimated total IKE values from a 24-hour  
685 SPIKE regression model (blue dots). The dark black line represents the best fit line between the  
686 4239 observed and estimated data points. The dashed line represents a perfect forecast ( $y=x$ ).

687

688 **Figure 4:** Evaluation of SPIKE model's skill during the 1990-2011 training interval. Plot of  
689 shared variance over forecast hour (panel A) and mean absolute error over forecast hour (panel  
690 B) for total IKE. The blue line represents these metrics between the observations and the SPIKE  
691 model at each forecast hour. The red line represents these metrics between a persistence  
692 forecast and the observed IKE value a certain number of hours later.

693

694 **Figure 5:** Percent reduction of mean squared error (MSE) for the SPIKE model during the 1990-  
695 2011 training interval with respect to persistence. A reduction of MSE is plotted as a positive

696 percentage, indicating improved model skill. The model's improvement over persistence is  
697 significant at the one-sided  $p=0.05$  level for all forecast hours greater than or equal to 24 hours  
698 and at the  $p=0.01$  level for all forecast hours greater than or equal to 30 hours.

699  
700 **Figure 6:** Evaluation of SPIKE model's skill during the 2012 Atlantic Hurricane season. Panel A  
701 depicts a plot of shared variance over forecast hour for total IKE measurements. More  
702 specifically, the blue line is the shared variance between the SPIKE model and observed total  
703 IKE measurements during the training interval of 1990 and 2011 reproduced from Figure 4a, the  
704 green line is the shared variance between the validation SPIKE model and observed total IKE  
705 values for all storms during the 2012 season, and the magenta line is the shared variance  
706 between observations and persistence during the 2012 season. Panel B depicts mean absolute  
707 error over forecast hour for total IKE. The blue line represents the mean error between the  
708 observations and the SPIKE model during the training period as reproduced from figure 4b. The  
709 green line represents the mean error of the validation SPIKE model for all storms in the 2012  
710 season. Finally, the orange line represents the mean error of the validation SPIKE model for the  
711 2012 season, excluding the final 3 days of Hurricane Sandy's lifecycle.

712  
713 **Figure 7:** Percent reduction of mean squared error (MSE) for the SPIKE model during the 2012  
714 season, excluding the final seventy-two hours of Hurricane Sandy's lifecycle, with respect to a  
715 persistence forecast. A reduction of MSE is plotted as a positive percentage, indicating  
716 improved skill. The model has significantly lower MSE than persistence at the  $p=0.05$  level for  
717 all forecast hours greater than or equal to 48 hours.

718

719

720

721 **Tables and Figures**

722

Variable	Definition	Units
PIKE	persistence of IKE	TJ
dIKE12	previous 12hr change of IKE	TJ
VMAX	maximum sustained wind speed	kts
dV12	previous 12hr change of VMAX	kts
VMPI	Difference between maximum potential intensity and VMAX	kts
LAT	latitude of storm's center	°N
LON	longitude of storm's center	-°W
DTL	distance to nearest landmass	km
UMOT	zonal translational storm motion	m·s <sup>-1</sup>
VMOT	meridional translational storm motion	m·s <sup>-1</sup>
MSLP	minimum sea level pressure	hPa
PENV	average surface pressure ( <i>averaged from r=200-800km</i> )	hPa
VORT	850 hPa vorticity ( <i>r=0-1000km</i> )	10 <sup>-7</sup> s <sup>-1</sup>
D200	200 hPa divergence ( <i>r=0-1000km</i> )	10 <sup>-7</sup> s <sup>-1</sup>
SHRD	850-200 hPa shear magnitude ( <i>r=200-800km</i> )	kts
SHTD	850-200 hPa shear direction ( <i>r=200-800km</i> )	°
SHDC	SHRD but relative to 850 hPa center with vortex removed ( <i>r=0-500km</i> )	kts
RHLO	850-700 hPa relative humidity ( <i>r=200-800km</i> )	%
RHMD	700-500 hPa relative humidity ( <i>r=200-800km</i> )	%
T150	150 hPa temperatures ( <i>r=200-800km</i> )	°C
RD20	ocean depth of 20°C isotherm	m
RD26	ocean depth of 26°C isotherm	m
OHC	ocean heat content	kJ·cm <sup>-1</sup>
SST	sea surface temperatures	°C
EPSS	average difference between lifted surface parcel $\theta_e$ and environment $\theta_{es}$ ( <i>r=200-800km</i> )	°C
TWAC	850 hpa symmetric tangential wind ( <i>r=0-600km</i> )	m·s <sup>-1</sup>
TADV	low-level temperature advection by thermal wind ( <i>r=0-500km</i> )	10 <sup>-6</sup> s <sup>-1</sup>
REFC	relative eddy momentum flux ( <i>r=100-600km</i> )	m·s <sup>-1</sup> ·day <sup>-1</sup>
PEFC	planetary eddy momentum flux ( <i>r=100-600km</i> )	m·s <sup>-1</sup> ·day <sup>-1</sup>
SDAY	time after tropical storm genesis	days
PDAY	time from peak of season (Sept. 10)	days

723

724 **Table 1:** Variables considered for use in the SPIKE models. Many of the variables (e.g. RHLO,  
725 SHRD) originated from SHIPS and are averaged over specific areas as noted. Others were  
726 specifically created from observations for the SPIKE model. Not all of these variables are used  
727 in the final models, as many of the regression coefficients fail significance tests in the backward  
728 screening methodology.

729

730

731

732

733

734

735

736

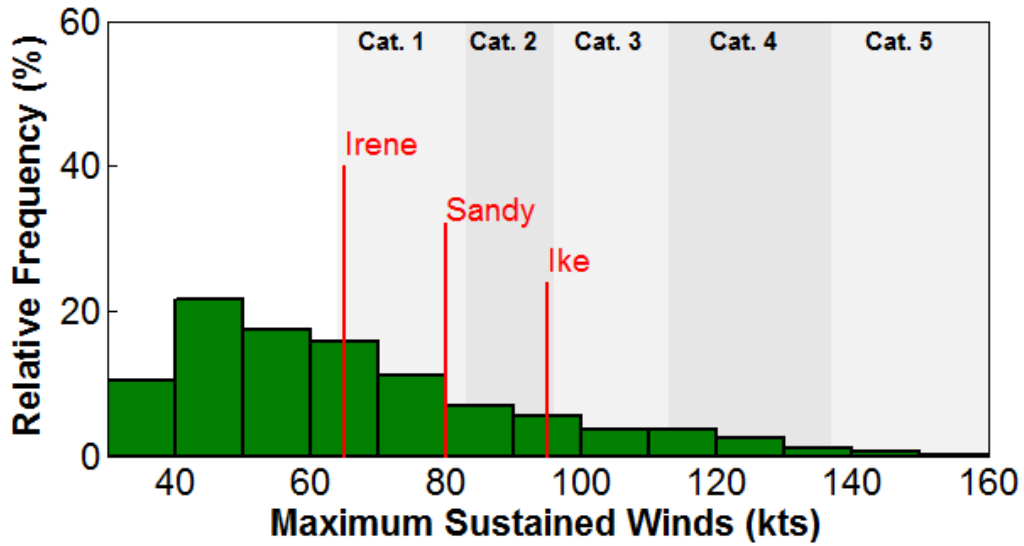
737

Variable	Forecast Hour				
	12hr	24hr	36hr	48hr	72hr
PIKE	-0.53	-0.70	-0.72	-0.70	-0.70
dIKE12	0.11	<i>0.02</i>	<i>0.02</i>	<i>0.00</i>	<i>-0.01</i>
RHLO	-0.13	-0.19	-0.22	-0.23	-0.25
SHRD	0.06	0.11	0.12	0.13	0.13
DTL	0.14	0.15	0.15	0.14	0.15
D200	0.12	0.13	0.12	0.12	0.11
MSLP	-0.26	-0.37	-0.39	-0.40	-0.41
VORT	0.16	0.19	0.20	0.20	0.20
LAT	0.24	0.30	0.33	0.34	0.36
RD26	0.11	0.11	0.10	0.10	0.09
EPSS	0.06	0.08	0.09	0.09	0.11
PENV	-0.08	-0.10	-0.13	-0.14	-0.18
REFC	0.07	0.08	0.07	0.05	<i>0.04</i>
PDAY	-0.08	-0.10	-0.11	-0.10	-0.08
<b>Sample Size</b>	4814	4239	3756	3341	2657
<b>Shared Variance</b>	13%	25%	39%	43%	54%

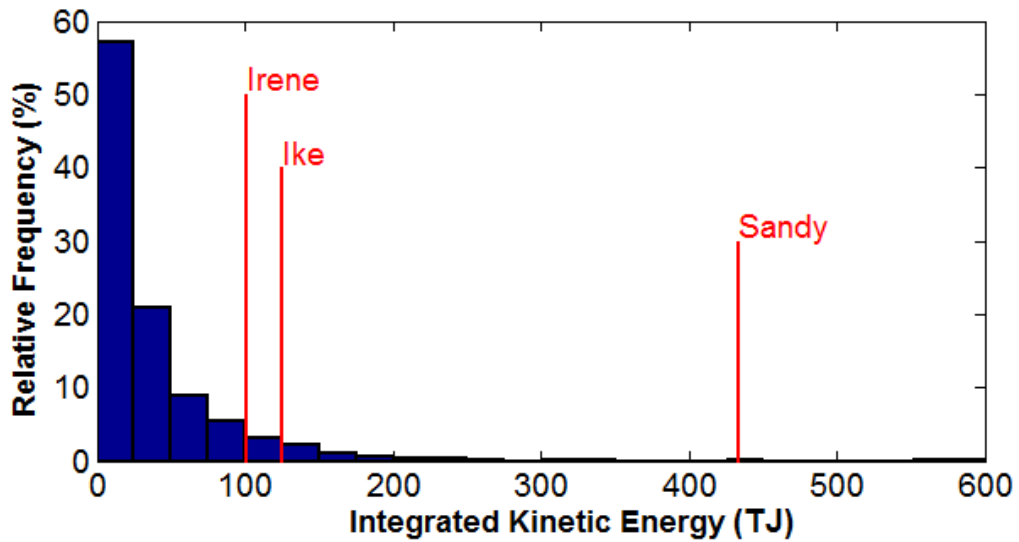
738  
739  
740  
741  
742  
743

**Table 2:** Regression coefficients for each predictor in the SPIKE model. The coefficients listed in a non-italicized font are significant at 99% for that forecast hour. Sample size for the training interval of 1990 to 2011 is shown below. Finally, shared variance between the SPIKE regression model, and observed kinetic energy changes are listed in the bottom row.

A)



B)



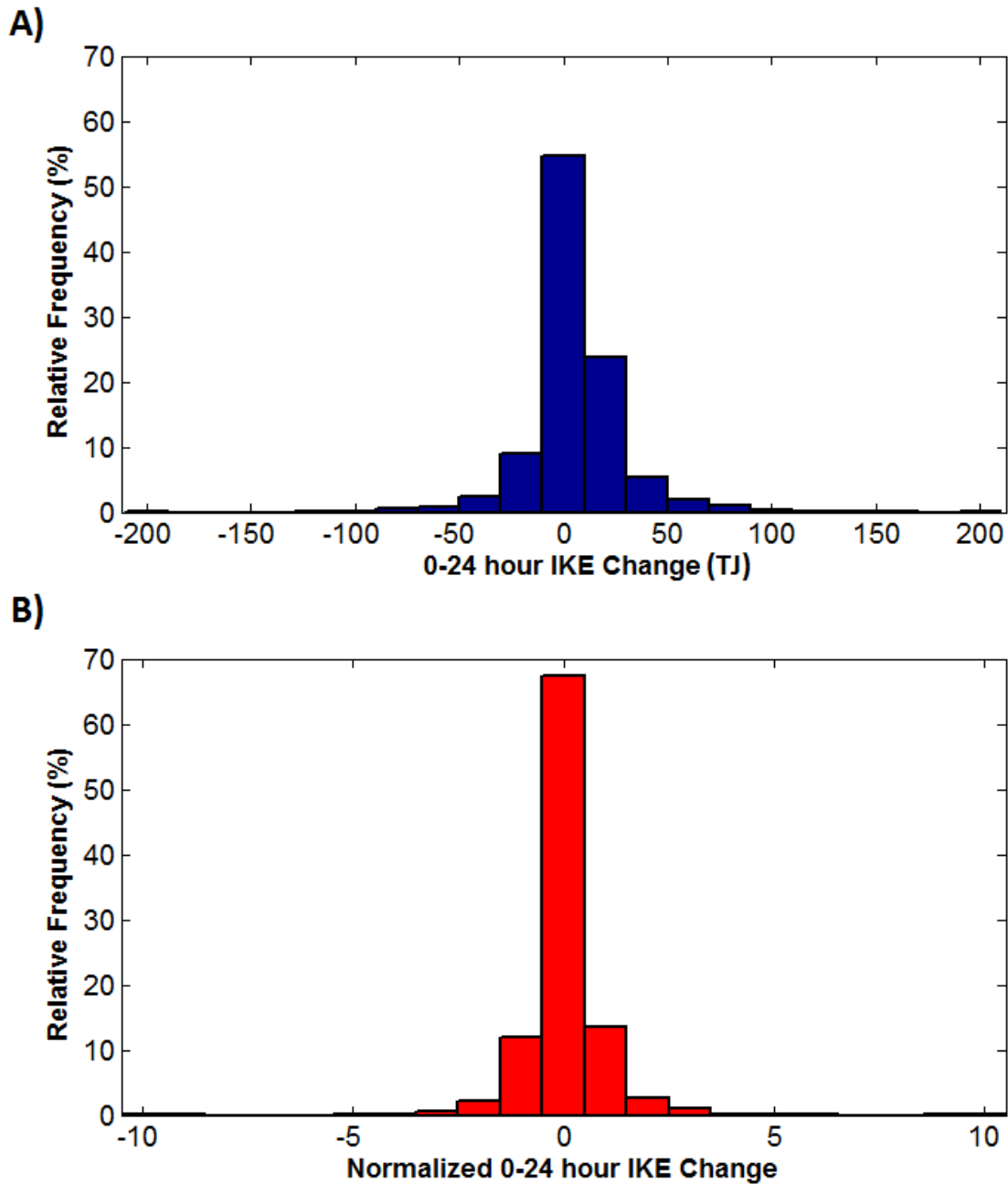
744  
745

**Figure 1:** Relative frequency distribution of six-hourly VMAX (panel A) and IKE (panel B) measurements in Atlantic TCs between 1990 and 2011. This sample includes 5498 fixes from 291 storms. Vertical lines are shown to indicate VMAX and IKE values for selected hurricanes just prior to a US landfall. The times of these IKE measurements are as follows: Ike 9/13/08 00Z; Irene 8/28/11 06Z; Sandy 10/29/12 18Z. The three storm points would fall in the top 45% of all TCs points in terms of VMAX and the top 7.5% of TCs in terms of IKE from 1990 through 2011.

753

754





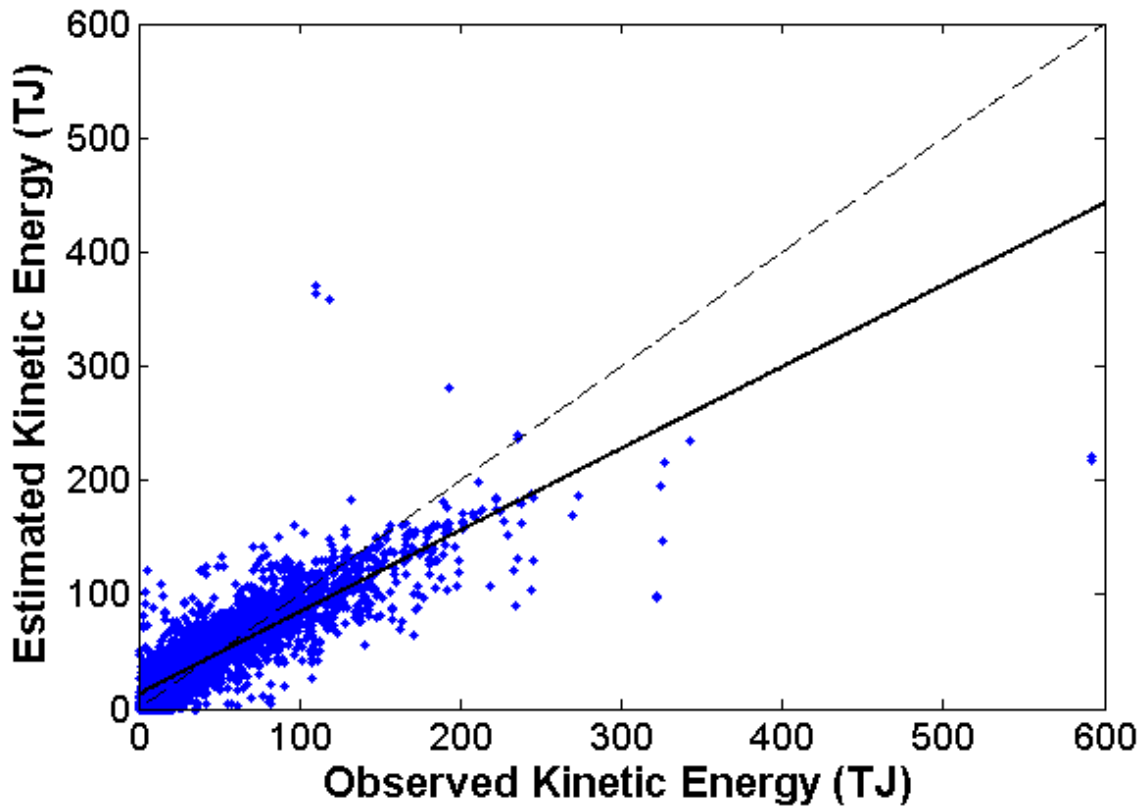
755

756 **Figure 2:** Relative frequency distribution of 0-24 hour IKE changes (panel A), and normalized 0-  
 757 24 hour IKE changes (panel B). The normalized changes of IKE at various forecast times is  
 758 used as the target predictand for the linear SPIKE regression models

759

760

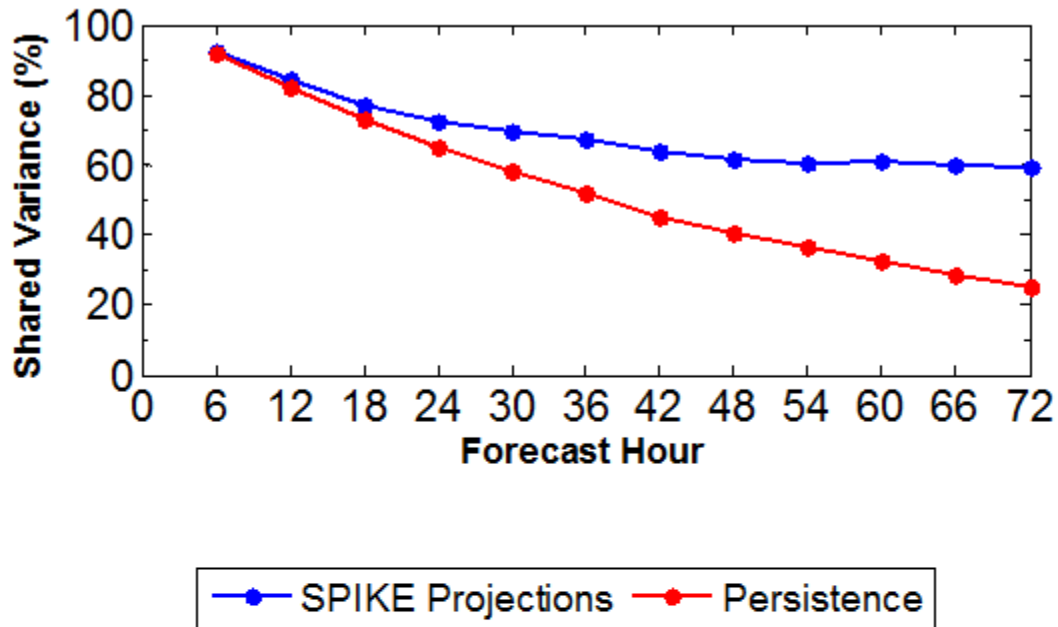
761



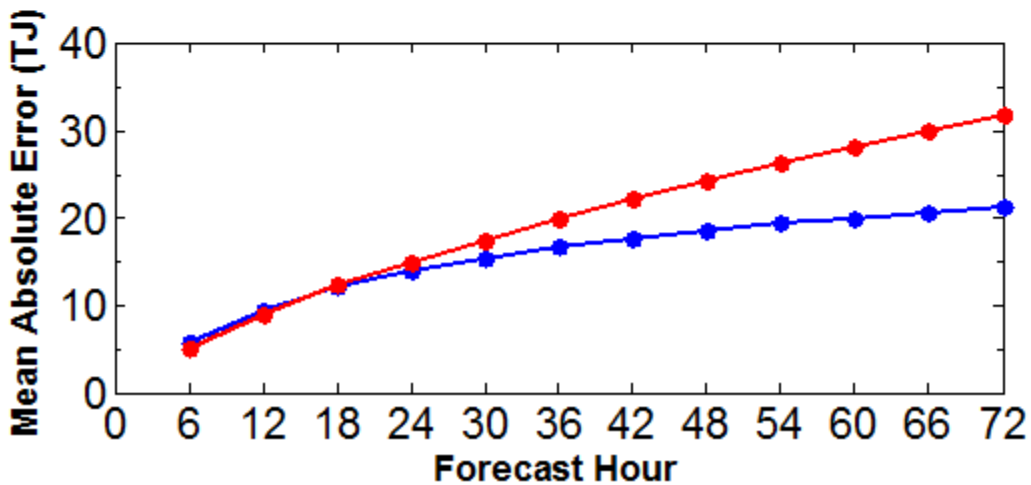
762  
763  
764  
765  
766  
767

**Figure 3:** Scatter plot of observed total IKE values vs. estimated total IKE values from a 24-hour SPIKE regression model (blue dots). The dark black line represents the best fit line between the 4239 observed and estimated data points. The dashed line represents a perfect forecast ( $y=x$ ).

A)

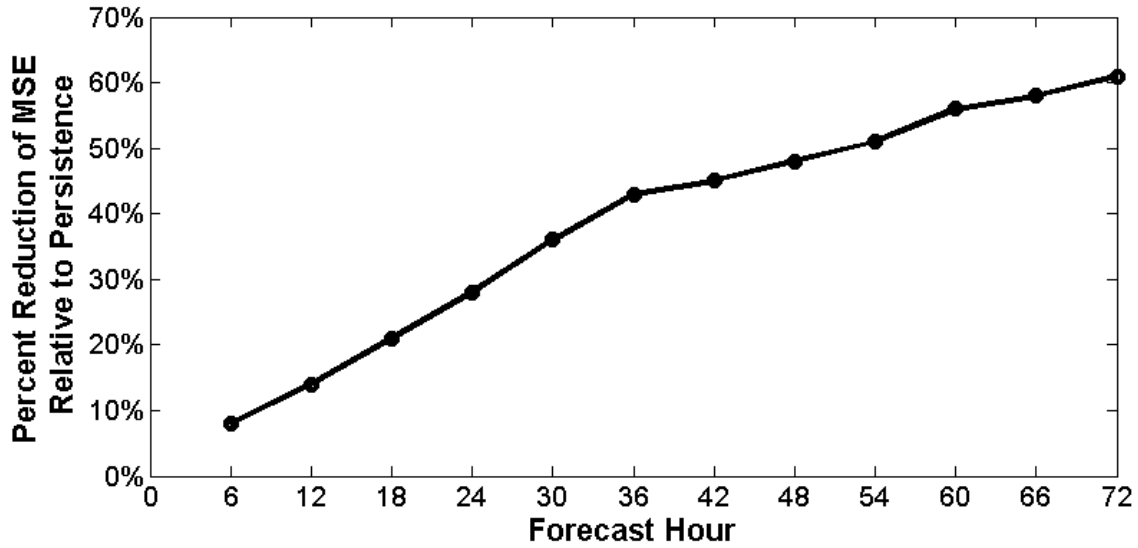


B)

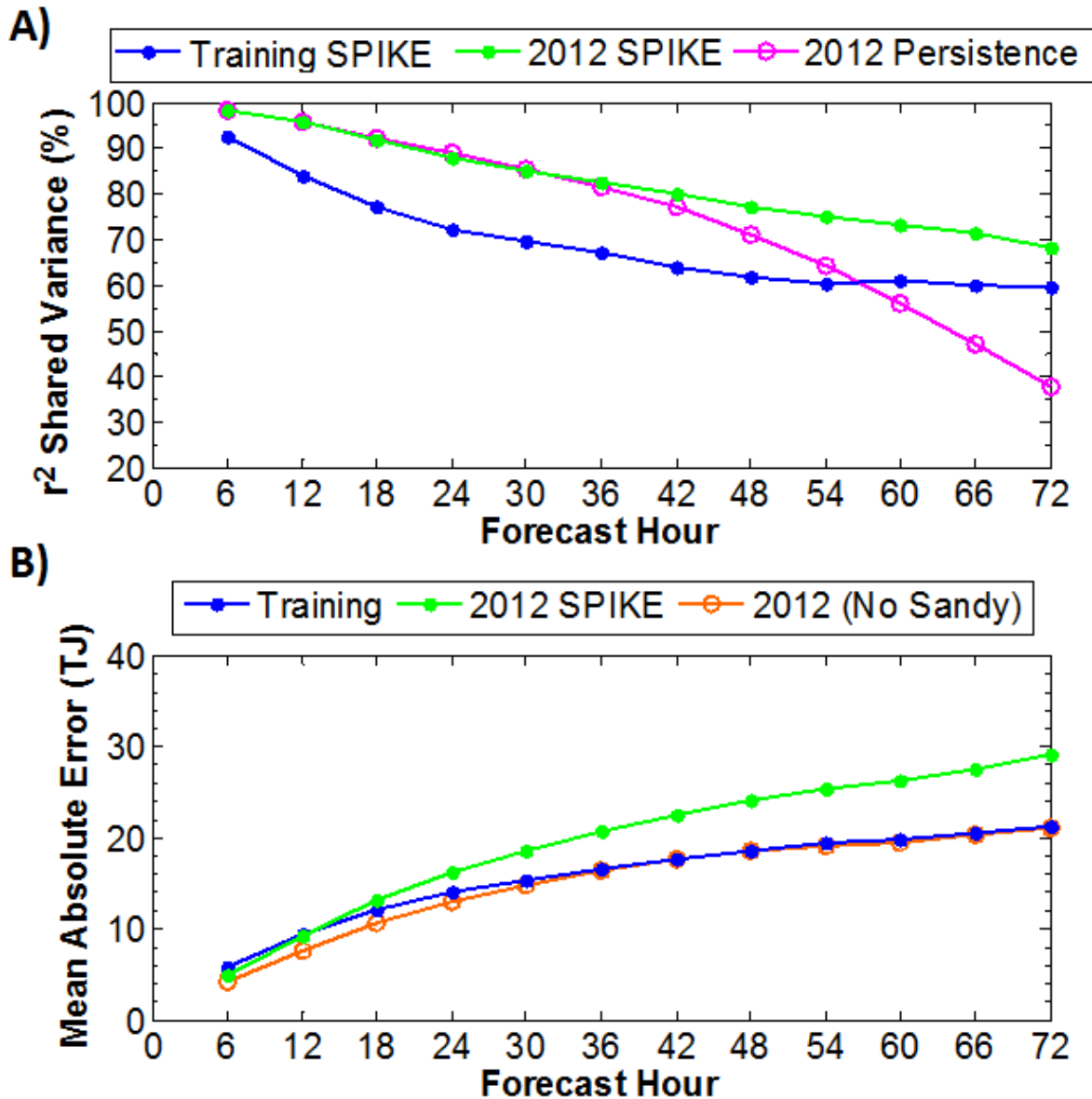


768  
769 **Figure 4:** Evaluation of SPIKE model's skill during the 1990-2011 training interval. Plot of  
770 shared variance over forecast hour (panel A) and mean absolute error over forecast hour (panel  
771 B) for total IKE. The blue line represents these metrics between the observations and the SPIKE  
772 model at each forecast hour. The red line represents these metrics between a persistence  
773 forecast and the observed IKE value a certain number of hours later.

774  
775  
776  
777  
778

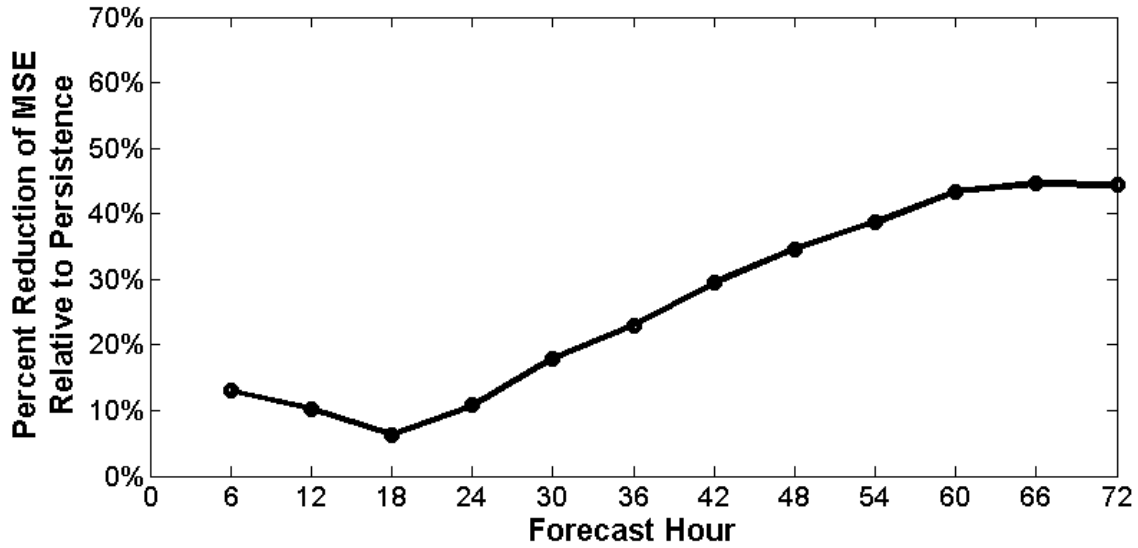


779  
 780 **Figure 5:** Percent reduction of mean squared error (MSE) for the SPIKE model during the 1990-  
 781 2011 training interval with respect to persistence. A reduction of MSE is plotted as a positive  
 782 percentage, indicating improved model skill. The model's improvement over persistence is  
 783 significant at the one-sided  $p=0.05$  level for all forecast hours greater than or equal to 24 hours  
 784 and at the  $p=0.01$  level for all forecast hours greater than or equal to 30 hours.  
 785  
 786  
 787  
 788  
 789



790  
 791 **Figure 6:** Evaluation of SPIKE model's skill during the 2012 Atlantic Hurricane season. Panel A  
 792 depicts a plot of shared variance over forecast hour for total IKE measurements. More  
 793 specifically, the blue line is the shared variance between the SPIKE model and observed total  
 794 IKE measurements during the training interval of 1990 and 2011 reproduced from Figure 4a, the  
 795 green line is the shared variance between the validation SPIKE model and observed total IKE  
 796 values for all storms during the 2012 season, and the magenta line is the shared variance  
 797 between observations and persistence during the 2012 season. Panel B depicts mean absolute  
 798 error over forecast hour for total IKE. The blue line represents the mean error between the  
 799 observations and the SPIKE model during the training period as reproduced from figure 4b. The  
 800 green line represents the mean error of the validation SPIKE model for all storms in the 2012  
 801 season. Finally, the orange line represents the mean error of the validation SPIKE model for the  
 802 2012 season, excluding the final 3 days of Hurricane Sandy's lifecycle.

803  
 804  
 805



806  
 807 **Figure 7:** Percent reduction of mean squared error (MSE) for the SPIKE model during the 2012  
 808 season, excluding the final seventy-two hours of Hurricane Sandy’s lifecycle, with respect to a  
 809 persistence forecast. A reduction of MSE is plotted as a positive percentage, indicating  
 810 improved skill. The model has significantly lower MSE than persistence at the  $p=0.05$  level for  
 811 all forecast hours greater than or equal to 48 hours.  
 812